2020

EXTRACELLULAR MATRIX NANOPARTICLES EFFECTS ON THE LUNG IN VIVO

Brittaney E. Ritchie
Virginia Commonwealth University

EXTRACELLULAR MATRIX NANOPARTICLES EFFECTS ON THE LUNG IN VIVO

A thesis submitted in partial fulfillment of the requirements for the degree of Master of Science in Biomedical Engineering at Virginia Commonwealth University.

By
BRITTANEY RITCHIE
B.S. Biology, Randolph-Macon College, 2016

Director: Rebecca L. Heise, Ph.D.,
Associate Professor and Undergraduate Program Director, Department of Biomedical Engineering

Virginia Commonwealth University
Richmond, Virginia
May, 2020

Acknowledgements

I would like to thank several people who I will forever be indebted to for their support in my master thesis journey. I would like to first thank my boyfriend, Mitch Ludwig, who was a shoulder for me to lean on in more ways than one. I would like to thank my advisor and mentor, Dr. Rebecca Heise. I am so grateful that she allowed me to be part of her lab and to take the lead of several challenging projects. I couldn't have made it through my work without her encouragement and countless guidance. The Heise Lab was an extension of her encouragement and I would like to give a special thanks to Dr. Beth Young. Dr. Young was/is always ready to answer any questions I had and without her I would be a ball of stress. I would also like to thank my undergraduate students, Anisha Beladia and Casie Slaybaugh, for all their help with progressing my investigations further. Finally, I would like to thank the rest of my friends and family who have made this achievement possible.

TABLE OF CONTENTS

LIST OF TABLES

LIST OF FIGURES

LIST OF ABBREVIATION AND SYMBOLS

ζ-potential	zeta potential
ARDS	Acute Respiratory Distress Syndrome
ATI	Alveolar Epithelial Cell Type I
ATII	Alveolar Epithelial Cell Type II
BALF	Bronchoalveolar Lavage Fluid
ECM	Extracellular Matrix
IP	Intraperitoneal
IT	Intratracheal
LPS	Lipopolysaccharide
MMP	Matrix Metalloproteinases
PEEP	Positive End Expiratory Pressure
PIP	Peak Inspiratory Pressure
PBS	Phosphate-buffered Saline
PLECM	Porcine Lung Extracellular Matrix
S/ECM	Saline/Extracellular Matrix Nanoparticles
S/S	Saline/Saline (Control)

ABSTRACT

EXTRACELLULAR MATRIX NANOPARTICLES EFFECTS ON THE LUNG IN VIVO

By Brittaney Ritchie

A thesis submitted in partial fulfillment of the requirements for the degree of Master of Science in Biomedical Engineering at Virginia Commonwealth University.

Virginia Commonwealth University, 2020

Director: Rebecca L. Heise, Ph.D.,

Associate Professor, Department of Biomedical Engineering

Acute respiratory distress syndrome (ARDS) is a life-threatening condition that causes diffuse alveolar damage and a loss of the extracellular matrix (ECM). This leads to pulmonary edema and lung function deterioration. Our lab has created decellularized porcine lung, electrosprayed ECM nanoparticles that have been previously shown to have pro-regenerative capabilities *in vitro*.

In this study, the ECM nanoparticle effects on young murine lungs were tested i*n vivo.* An ECM nanoparticle suspension, previously used for the *in vitro* studies, was aerosolized intratracheally into the lungs using a microsprayer. 24 hours later, the lung mechanics, bronchoalveolar lavage fluid, and histology were evaluated.

The ECM nanoparticles had no significant damaging effects to the lungs and were comparable to the control groups. Further studies are being done to establish an ARDS model using the ECM nanoparticle treatment.

CHAPTER 1

INTRODUCTION

1.1 Lung Anatomy and Physiology

The respiratory system is responsible for the gas exchange of oxygen and carbon dioxide. The inspired air from the environment brings in oxygen that can be passed into the bloodstream, where it can circulate to the cells in the rest of the body. When breathing takes place, air passes through the respiratory tract, which divides distally into two specific zones: the conducting zone and the respiratory zone (Figure 1).[1]

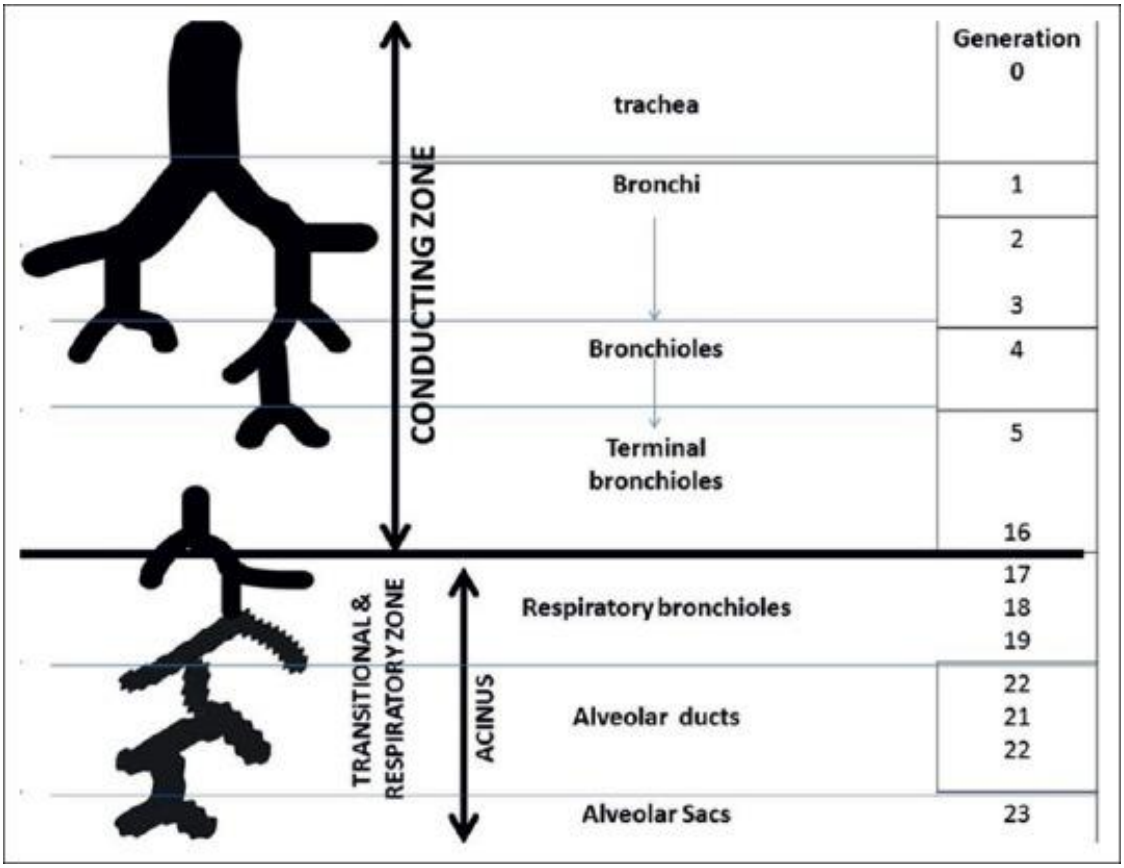

Figure 1. Diagram of the conducting and respiratory airways.[2]

1.2 Conducting and Respiratory Zones

The conducting zone provides a continuous passageway for air to move into and out of the respiratory airways. The main function of the conducting zone is not only to provide pulmonary ventilation, but also to warm, moisten, and filter the air prior to reaching the gas exchange region. Filtration of small inhaled particles occurs by the mucus-secreting and ciliated cells that line the conducting zone. This zone is comprised of the nose, nasopharynx, larynx, trachea, bronchi, bronchioles, and terminal bronchioles. The structure of the lungs involves twenty-three divisions into increasingly smaller airways from the trachea to the alveoli in the respiratory zone.[1,2,3]

The respiratory zone is comprised of the respiratory bronchioles, alveolar ducts, and alveolar sacs. Each of these structures participates in gas exchange and are lined with alveoli at varying amounts. Alveoli are sparsely located along the walls of the respiratory bronchioles, and the alveoli lining the alveolar ducts are sacs are more numerous in comparison.[1]

1.3 Alveolar Structure and Function

A large portion of the lung, approximately 90% of its total volume, is comprised of the alveolar region where the alveoli reside and where gas exchange occurs (Figure 2).[4] Separating each adjacent alveoli is the alveolar wall or interalveolar septum. The interalveolar septum not only separates adjacent alveoli, but also separates the alveolar air space from the blood-filled capillaries.[1,4,5]

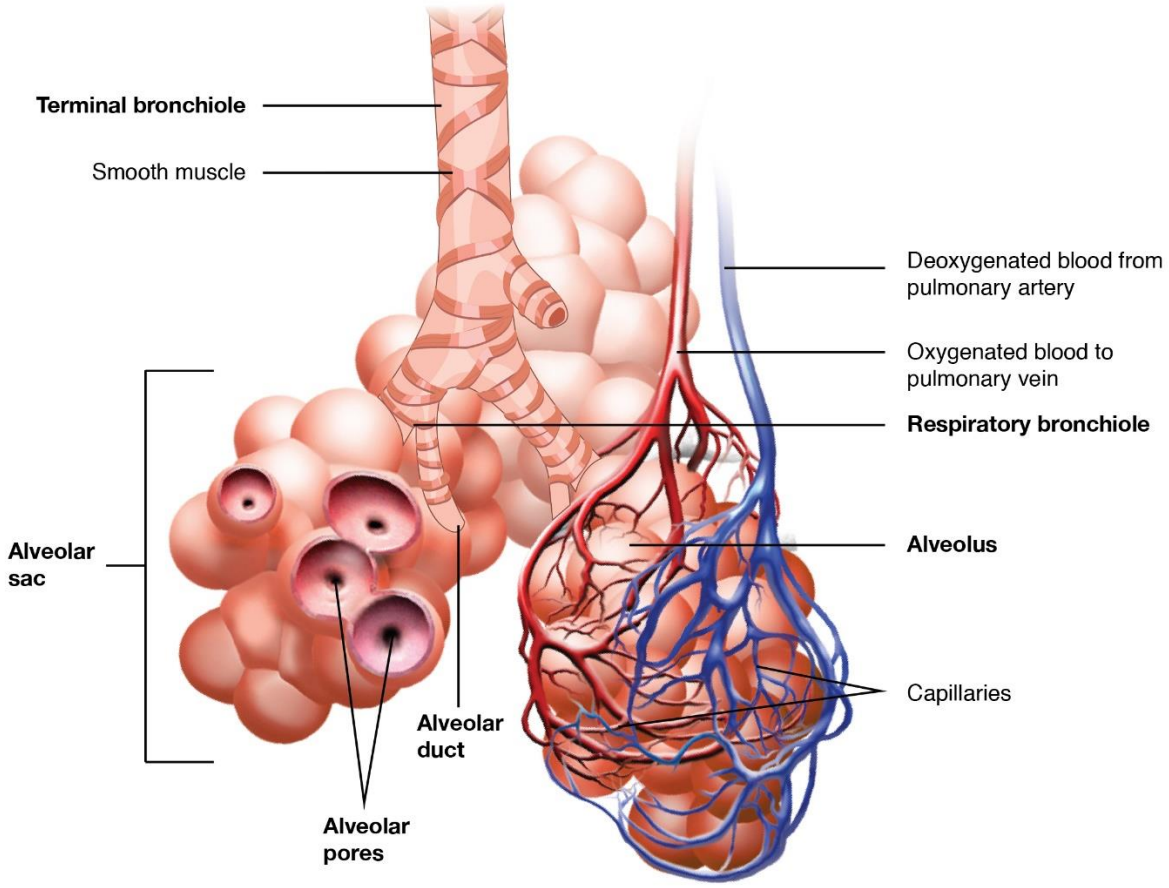

Figure 2. Diagram of lung alveolar structure.[5]

The interalveolar septum is comprised of two types of alveolar epithelial cells: type I (ATI) and type II alveolar epithelial cells (ATII). ATIs are thin, squamous cells that line the alveolar septum and are known to maintain the homeostasis of the alveoli.[4,6,7,8] ATIIs are cuboidal cells that function in renewal and repair. ATIIs synthesize and secrete surfactants, which reduce the surface tension of at the air-liquid interface; and serve as the alveolar progenitor cells. [4,7,8,9] ATIIs differentiate into ATI cells when damage to ATIs occur.[4,7,8] Together, these two cell types form the epithelial barrier and prevent fluids from entering the alveoli.

1.4 Lung Extracellular Matrix

The extracellular matrix (ECM) is necessary for normal functionality, physical support, and delivers cues that drive cellular differentiation.[10] In the lung, the ECM determines airway structure and is organized into the basement membrane and interstitial spaces.[10-12] The basement membranes are thin sheets of glycoproteins found under the epithelial and endothelial cell layers that surround muscle, fat, and peripheral nerve cells.[10,12] The interstitial spaces form the parenchyma of the lung which maintains the cohesiveness and biomechanical characteristics of the lung (Figure 3).[10,12]

A major portion of the lung's ECM protein content is made up of collagen; types I, II, III, V, and XI.[12, 13] Type I collagen is within the alveolar wall, type III is within the alveolar septa and interstitium of the alveoli, and type IV is within the epithelial and endothelial basement membranes.[13] The ECM is also made up of a fibrous proteins, glycoproteins, and proteoglycans.[10, 12, 14]

It is important to maintain the integrity of the lung in order to maintain proper lung function. Thus, it is important to maintain normal lung ECM and treat any lung ECM damage that can often be a result of pulmonary diseases.

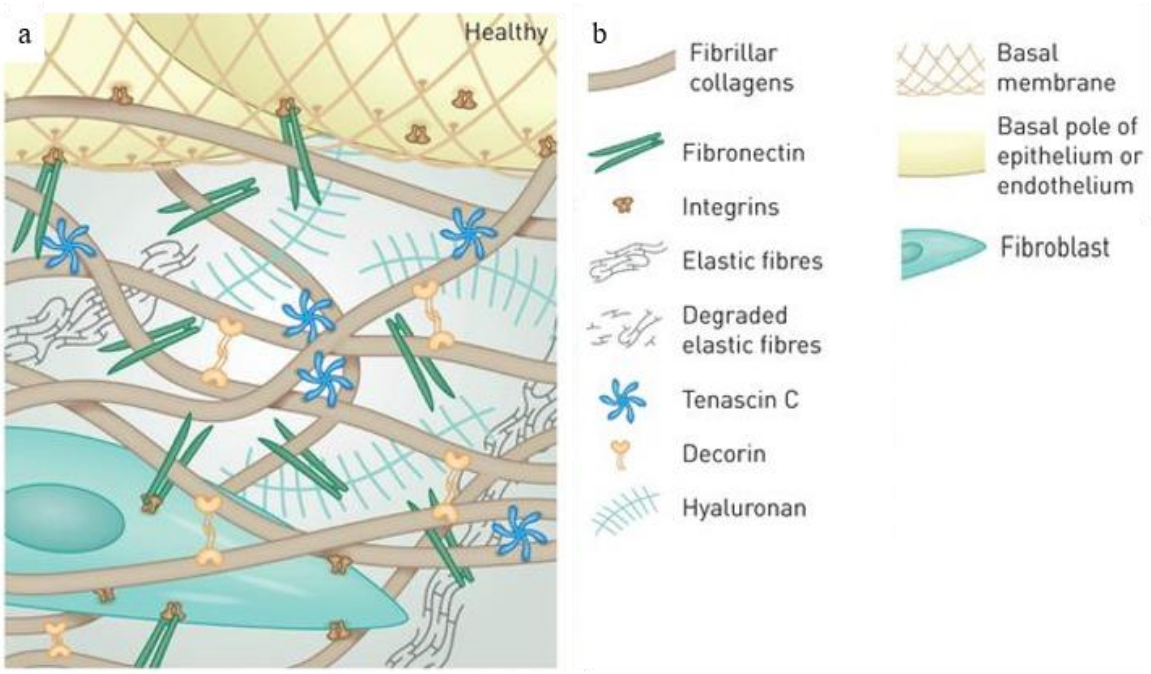

Figure 3. Diagram of the healthy lung ECM. a. The healthy lung ECM contains fibroblasts, collagens, elastin, and fibronectin. b. Legend of molecules and cell types.[12]

CHAPTER 2

ACUTE RESPIRATORY DISTRESS SYNDROME

2.1 Acute Respiratory Distress Syndrome

Acute respiratory distress syndrome (ARDS) is a life-threatening condition with a high mortality rate that is usually caused by pneumonia, severe sepsis, aspiration of gastric contents, or major trauma.[15,16] This syndrome is characterized by the filling of the alveoli with protein-rich pulmonary edema, which leads to hypoxemia and reduced lung compliance.[16, 17] Diffuse alveolar damage occurs, and the injury to the alveolar capillaries disrupts the endothelial barrier and causes damage to the ECM.[18] This alveolar-capillary barrier damage and increased vascular permeability allow for fluid to fill the alveoli. As the air space fills with fluid, lung function deteriorates, and gas exchange is impaired.[16, 17, 18]

2.2 Macrophage Phenotypes

The first responders of the immune response are the macrophages. Macrophages can either phagocytose foreign objects or initialize an immune cascade by releasing cytokines that can recruit other immune cells to the injury site.[28] Macrophages have two polarization states: the classically activated, pro-inflammatory M1 state and the alternatively activated, anti-inflammatory M2 state.[19] M1 macrophages are responsible for inflammatory signaling, and M2 macrophages contribute to tissue healing process.[20] Previous studies have observed that the M1 macrphages kill infectious organisms and virus-infected cells; however, this can come at the price

of resulting collateral tissue damage. In healty issue, macrophages tend to polarize to the M2 phenotype, which has been shown to provide growth factors and heal damaged tissues.[21]

In ARDS, when alveolar macrophages are activated, inflammatory cytokines, such as IL-1β, TNF-α, IL-6, and IL-8, are secreted. These cytokines stimulate chemotaxis and activate neutrophils.[16]

2.3 Neutrophil-Dependent Injury

Neutrophils are part of the immune system and are types of white blood cells that play a vital role in the defense against infection.[22] Neutrophils become activated and are recruited to the injury site where the infection or trauma to the body has occurred. However, the immune system can become hyperactivated as a response to infection or trauma, and activated neutrophils have the potential to cause cell-mediated damage at remote organs.[23]

In the case of ARDS, significant amounts of neutrophils accumulate in the lung microvasculature and release several toxic mediators, such as proteases and pro-inflammatory cytokines, that damage the lung endothelial and alveolar epithelial regions (Figure 4). Both lung endothelial and alveolar epithelial damage must occur for the injury to be diagnosed as ARDS. Lung endothelial damage is the first to occur and endothelial and epithelial damage is often caused by the influx of neutrophils. [16, 18, 23]

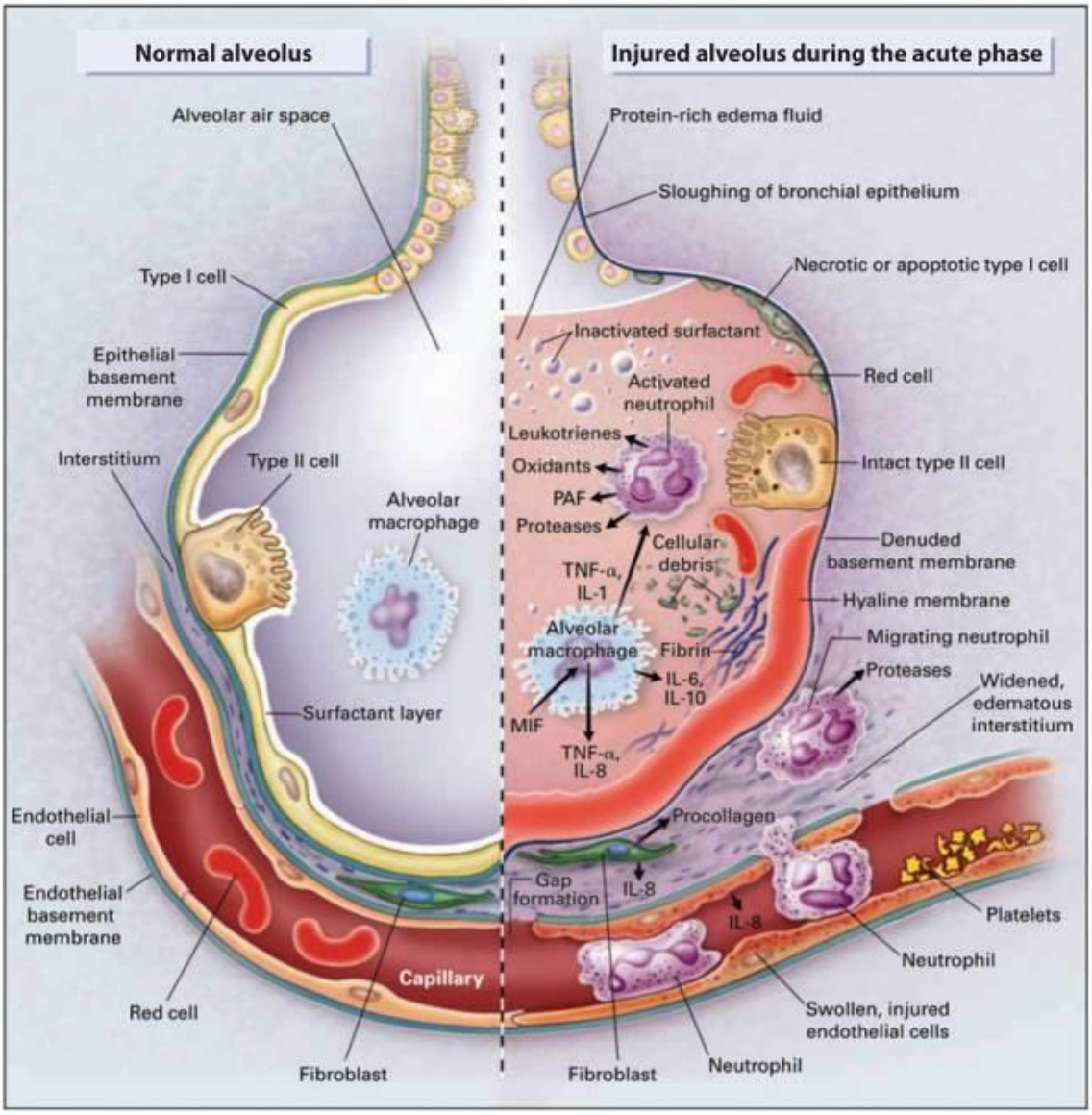

Figure 4. Overview of the pathogenesis of ARDS. *Left hand side*: The normal alveolus. *Right hand side*: The injured alveolus during the acute phase of ARDS. When alveolar macrophages are activated, inflammatory cytokines, such as IL-1β, TNF-α, IL-6, and IL-8, are secreted. These cytokines stimulate chemotaxis and activate neutrophils. Neutrophils adhere to the injured capillary endothelium and enter into the pulmonary edema filled interstitium; which then release several toxic mediators, such as proteases and other proinflammatory cytokines. This results in increased vascular permeability. [16]

2.4 ARDS ECM Damage

In order for the lung to function properly, the ECM integrity must be maintained. ARDS leads to damages and changes to the ECM which include: altered alveolar septa with lung fibrosis; increased amounts of collagen, elastic fibers, and fibronectin; and increased levels of matrix metalloproteinases (MMP).[18,24] MMPs can degrade all known components of the ECM which effects the regulation of cell growth, cell proliferation, cell survival, and cell migration.[18] Higher expressions of MMP-9, and in some cases MMP-2, are often seen in human patients and in animal models with ARDS and appears to be a central component of lung injury.[18,24] The underlying mechanism is not well understood; however, targeting the ECM, and thus the MMPs, may be critical for the development of potential therapies for ARDS.[18]

2.5 Treatment

Currently, there is no cure or effective therapeutic for ARDS. Treatments focus on supportive patient care and include providing respiratory support through mechanical ventilation and fluid management. The treatments tend to focus on the symptoms rather than the syndrome and are designed to: increase oxygen delivery, decrease oxygen consumption, and avoid further injury.[16, 25, 26] In addition to the high mortality rate associated with ARDS, patients who manage to survive have lasting health complications; thus, there is a need for further treatment options.

CHAPTER 3

EXTRACELLULAR MATRIX NANOPARTICLES

3.1 Extracellular Matrix Nanoparticles

Decellularized ECM is usually composed of proteoglycans, growth factors, and fibrous proteins, such as collagens, elastins, fibronectins, and laminins.[27,28] ECM is known to promote normal tissue repair due to their degradation products. The degradation products are known to have chemoattractant [29, 30, 31] and antimicrobial [31, 32, 33] properties, and these properties have been utilized in recent lung injury studies. Porcine urinary bladder ECM has been shown to promote epithelial wound repair and protect against pulmonary fibrosis.[34] In another study, inhaled porcine lung ECM microparticle (< 3 μm) solutions were shown to reduce oxidative damage in an acute lung injury model.[35] Previous studies in our lab have improved upon these recent studies by creating porcine lung ECM nanoparticles that maintain their pro-regenerative benefits and may improve lung deposition to the distal regions of the lung that are most affected by ARDS. [33]

3.2 ECM Nanoparticle Characteristics: Size

Current devices for aerosolized therapeutics have yet to be able to deposit necessary drugs throughout the total lung. For instance, devices such as the metered-dose inhalers and the dry powder inhalers are only able to deposit about 10-20% and 12-40% of the emitted drug dose to the lungs, respectively. [24, 36, 37] This may be partially due to the microparticle sized drugs that are often used in these inhalers. [38, 39] Particles delivered to the lung must have a diameter size range

of 260-500 nm in order to reach the alveoli. [40-42] The size of our ECM nanoparticles is 225 (± 67) nm, which is an optimal diameter size needed to reach the distal region of the lungs (Figure 5). [33]

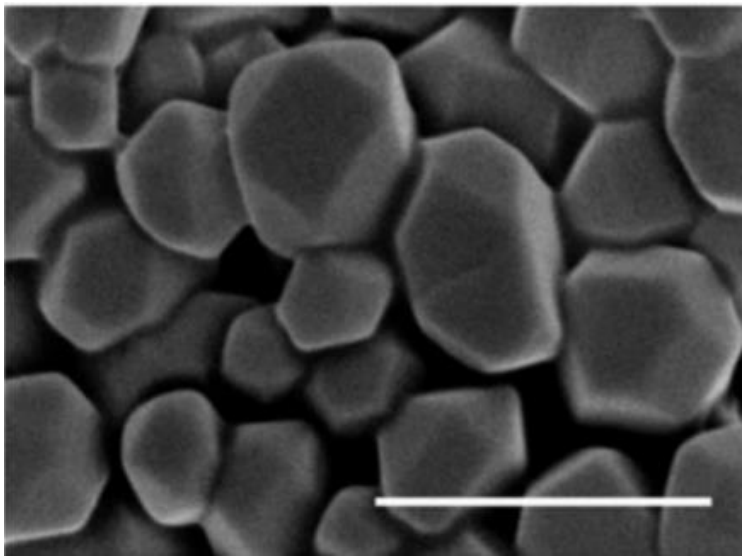

Figure 5. ECM nanoparticles. A scanning electron micrograph of the particles deposited on aluminum foil. Scale bar is 1 µm. This image was reproduced with permission from the Wiley Online Library. [33]

3.3 ECM Nanoparticle Characteristics: Surface Charge, Cytotoxicity & Pro-regenerative Effects

An indicator of improved biocompatibility and low cytotoxic effects is a negative surface charge, or ζ-potential, and studies in our lab have proven that the nanoparticles have a slightly negative charge and are not toxic *in vitro*. The nanoparticles increased the proliferation of lung epithelial cells, specifically A549 cells at 24 and 48 hours. The nanoparticles also increased the M2-type macrophage surface marker CD206 and decreased the M1-type macrophage surface marker CD11c; inducing a pro-regenerative macrophage phenotype when added to bone-marrow derived macrophages [33].

CHAPTER 4

RESEARCH DESIGN

4.1 Overview

The particle size, ζ-potential, and passive degradation of our ECM nanoparticles have previously been characterized.[33] In addition, the cytotoxicity and the ability to shift macrophages to a pro-regenerative phenotype have also been characterized *in vitro*.[33] However, our ECM nanoparticles have yet to be tested *in vivo*. We **hypothesized** that the nanoparticles would not negatively impact the lung mechanics or cause inflammation. To test this hypothesis, the nanoparticles were aerosolized into young murine lungs using a microsprayer at similar concentrations previously used *in vitro*.[33] 24 hours after ECM nanoparticle aerosolization into the lungs, the lung mechanics, bronchoalveolar lavage fluid (BALF) cell counts, and histology were evaluated.

4.2 Specific Aim

Specific Aim: Evaluate the lung mechanics, BALF cell counts, and histology after nanoparticle aerosolization into an *in vivo* murine model.

CHAPTER 5

IN VIVO STUDY

5.1 Rationale

In vivo testing was performed to ensure that the lungs remained unharmed when the nanoparticles were aerosolized within them. To ensure that the nanoparticles were safe to be used *in vivo*, the lung mechanics, cytological analysis, and histology were compared among a control group and 0.125 mg/mL ECM nanoparticle solution concentration that has been previously used *in vitro*.

5.2 Methods

* Adapted from [33], [43], and [47]

5.2.1 Decellularizing Porcine Lung Tissue

Porcine lungs were obtained from Smithfield-Farmland slaughterhouse to produce decellularized ECM powder. Decellularization was achieved with tracheal and vascular detergent perfusion of sterile 1x phosphate-buffered saline (PBS), 0.1% triton X-100, 2% sodium deoxycholate, 1M sodium chloride, and DNAse over 3 days in 4^{o}C. After decellularization, the lung should be clear and white. Large cartilaginous airways were removed, and the remaining alveolar and small airway structures were lyophilized for 48 hours before freeze-milling into a fine powder. The fine powder was stored at -20^{o}C until needed.

5.2.2 Nanoparticle Formation through Electrospray Deposition

PLECM powder was digested for 48 hours at room temperature in 80% v/v glacial acetic acid in ultrapure H_20. After 48 hours, the solution was drawn up in a 10 mL syringe fitted with a 26-gauge blunt needle (IntelliSpense) and attached to a syringe pump (Kent Scientific, GenieTouch™) set to 10 mL/hour. The syringe pump was placed on the top of a 1/2" Delrin® (polyoxymethylene) box with a hole drilled into it for the syringe to pass through. Inside the box, the blunt needle tip was connected to the voltage generator (Spellman CZE1000R) and grounded to aluminum foil located approximately 10 cm away from the blunt needle tip. The voltage difference, at 25 kV, between the blunt needle tip and aluminum foil caused nanoparticle formation through rapid liquid evaporation (Figure 6).

The nanoparticles were removed from the foil using sterile 1x PBS and lyophilized for 48 hours to form a powder. The nanoparticle powder was diluted using sterile 0.9% saline to 0.125 mg/mL protein concentration. Since the ECM nanoparticle solution begins to degrade after a month, fresh ECM nanoparticles for new solutions were made prior to each *in vivo* experiment.

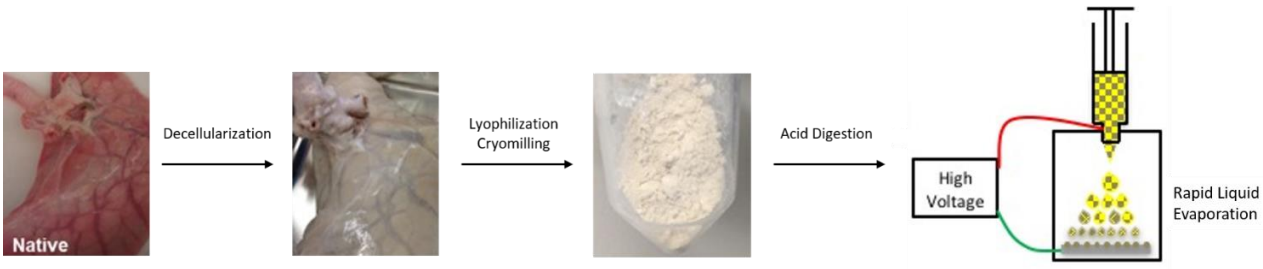

Figure 6. Overview of the process to produce ECM nanoparticles. Decellularized PLECM is acid digested and electroprayed into nanoparticles.

5.2.3 Animals

This study was approved by the VCU Institutional Animal Care and Use Committee (protocol number AD10000465). Wild type, young adult male and female C57BL/6 mice (age, 8-10 weeks; weight, 22-25 g; Charles River Laboratories) were used in these experiments. The mice were maintained at a constant temperature (23^{o}C) with free access to food and water under a 12-h light/dark cycle condition. All animal experiments were conducted in accordance with the IACUC University guidelines.

5.2.4 Treatment Groups

Each subject was randomized into the following treatment groups: saline/saline (S/S) or saline/ECM (S/ECM). An hour before treatment, 50 µL of 0.9% sterile saline was aerosolized intratracheally (IT) using a Penn-Century MicroSprayer® aerosolizer (Philadelphia, PA) (Figure 6). Treatment, either 50 µL of 0.9% sterile saline (control) or 50 µL of 0.125 mg/mL sterile ECM nanoparticle solution, was aerosolized IT using the MicroSprayer® aerosolizer. Each subject's recovery was monitored, and once responsive, the subjects were moved to the vivarium for 24 hours prior to mechanical ventilation (Figure 7).

5.2.5 Intratracheal Aerosolization

Prior to IT instillation, subjects were anesthetized with an intraperitoneal (IP) injection of 80 mg/kg sodium pentobarbital. Each anesthetized subject was placed on a slanted board (45° from vertical) in the supine position and was supported by suture under the upper incisors.[44] The trachea was illuminated with a microscope lamp. Blunted forceps were used to help displace the

tongue for complete trachea exposure.[45] After a clear view of the trachea, the MicroSprayer® aerosolizer was used to aerosolize 50 µL of the 0.125 mg/mL ECM nanoparticle solution IT (Figure 6). Approximately 70 µL of solution was lost in the MicroSprayer® aerosolizer; thus, 70 µL of air was pushed behind the 50 µL of solution to ensure complete delivery into the lungs. Once the solution was sprayed, the subject was immediately taken off the support.

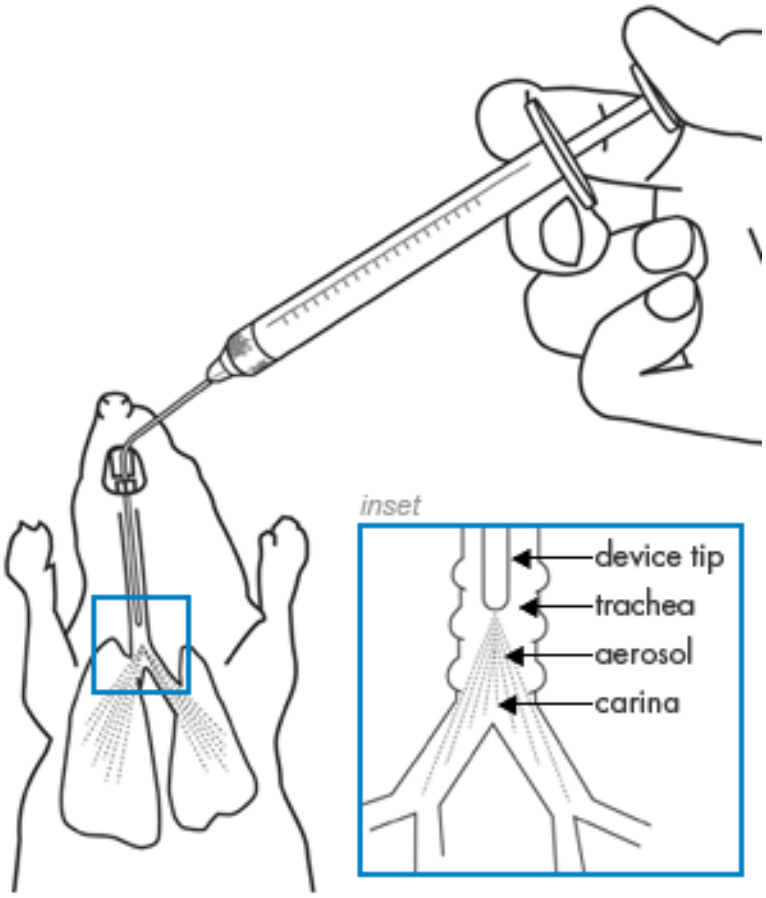

Figure 7. Solution aerosolization route using the Penn-Century MicroSprayer® aerosolizer. [46]

5.2.6 Mechanical Ventilation

24 hours after IT treatment, subjects were anesthetized with an IP injection of 80 mg/kg sodium pentobarbital prior to experimentation. The depth of subject anesthesia was monitored continuously using an electrocardiogram transducer monitor included in the FlexiVent small animal ventilation hardware (SCIREQ Scientific Respiratory Equipment Inc). To maintain an appropriate level of anesthesia over the course of intubations, sodium pentobarbital redoses of 40 mg/kg were administered as needed when a subject's heart rate increased by 10% compared to the baseline heart rate.

In addition to the anesthesia, the mechanical ventilation protocol required an IP administration of 0.8 mg/kg pancuronium bromide to prevent spontaneous breathing that could skew mechanical data.

In order to collect lung mechanic data, subjects were mechanically ventilated for 10 minutes on non-injurious settings with 30 cmH_20 peak inspiratory pressure (PIP), 150 breaths per minute, 3 cmH_20 positive end expiratory pressure (PEEP) using a FlexiVent small animal ventilator (SCIREQ) (Figure 8).

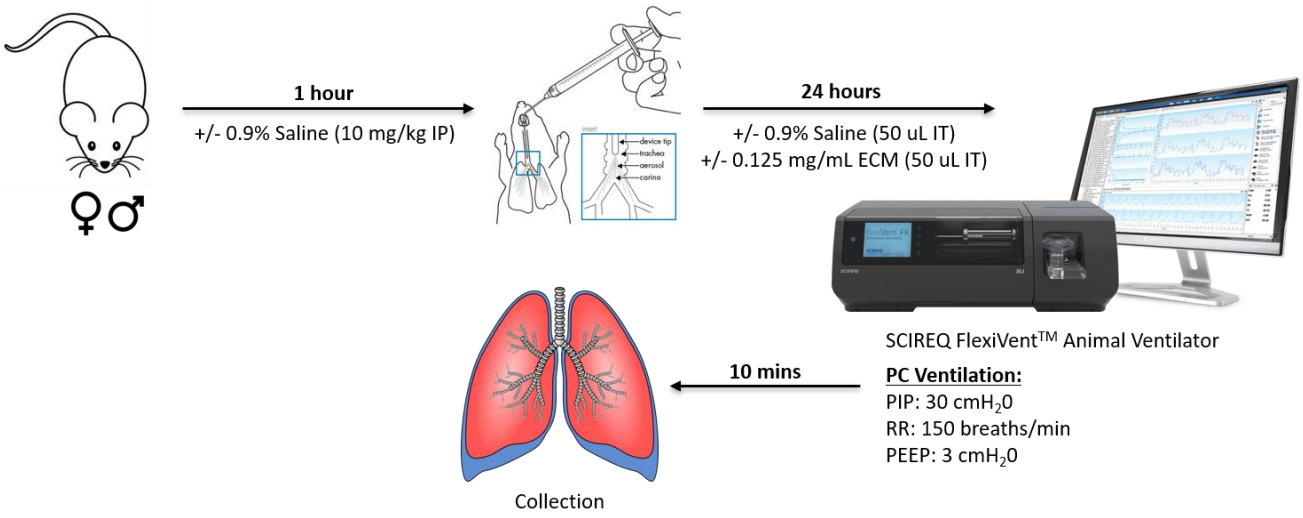

Figure 8. Overview of the *in vivo* studies testing the effects of the ECM nanoparticle solution at 0.125 mg/mL.

5.2.7 Lung Mechanics

Snapshot-150 v7.5 and Deep Inflation v7.5 were performed using the included FlexiWare software package (SCIREQ). Snapshot measures lung tissue compliance: resistance, compliance, and elastance. Deep inflation measures the inspiratory capacity or total lung capacity.

5.2.8 Bronchoalveolar Lavage

A bronchoalveolar lavage was performed three times using 500 µL of cold, sterile 1x PBS each time. The PBS was instilled into the lungs using a tracheal cannula. Lungs were slowly inflated and deflated to ensure no airway rupturing. 1.5 mL of total bronchoalveolar lavage fluid (BALF) per subject was obtained using this technique.

5.2.9 BALF Cytology

BALF was centrifuged at 400 × g, 4 °C for 10 minutes. The supernatant was removed, and the cell pellet was re-suspended in 3 mL of ammonium-chloride-potassium lysing buffer to lyse and remove the red blood cells. The solution was centrifuged at 400 × g, 4 °C for 10 minutes and the supernatant was removed. The cell pellet was re-suspended in 1.5 mL of sterile 1x PBS and 90 µL was removed for total cell counts. The solution was centrifuged a final time at 400 × g, 4 °C for 10 minutes and the supernatant was removed. The cell pellet was re-suspended in 300 µL of sterile 1x PBS.

Using a cytospin device (Shandon), cells were then mounted onto glass slides. Cells were stained using a 3 Diff-Quik solutions staining kit and cover-slipped. Cell populations were then analyzed using microscopy (Olympus), and the ratios of lymphocytes, monocytes, and neutrophils were determined.

5.2.10 Lung Histology

Left lungs fixed with 4% paraformaldehyde, sectioned, and H&E stained. Stained slides were imaged using an Olympus IX71 Microscope (Olympus).

5.2.11 Statistical Analysis

GraphPad Prism 6 statistical analysis software were used for all quantitative experimental studies. All quantitative experimental studies were performed with a minimum of n = 2. Lung mechanic statistics were performed using an unpaired t-test with Welch's correction. BALF

cellularity percentage statistics were performed using a two-way ANOVA test. P values of < 0.05 were considered significant.

5.3 Results

5.3.1 Lung Mechanics

Lung mechanics of both the S/S group (control) and the S/ECM group were measured 24 hours after IT aerosolization using the SCIREQ FlexiVent software. The lung resistance of the S/ECM group was slightly more resistance than the S/S group. The inspiratory capacity of the S/ECM group lungs was slightly lower than the S/S group. However, the lung resistance, compliance, elastance, and inspiratory capacity showed no significant difference between the two groups (Figure 9).

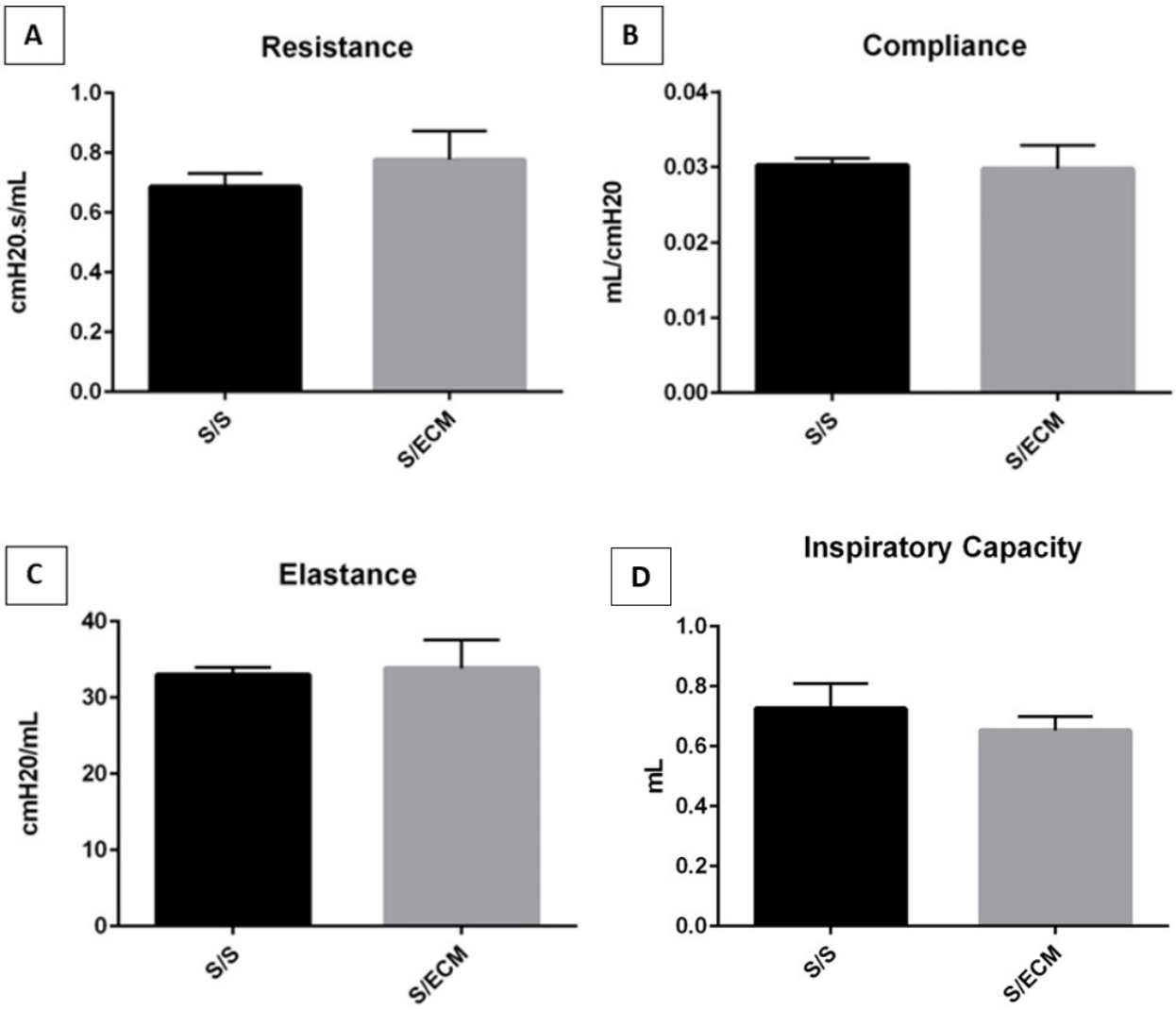

Figure 9. Lung mechanics. There is no significant difference in lung resistance, compliance, elastance, or inspiratory capacity between the control group and S/ECM group. A. Lung resistance. Although the lungs of the S/ECM group were slightly more resistant compared to the control, S/S, group, there was no significant difference in lung resistance between the two. B. Lung compliance. There was no significant difference in lung compliance between the two. C. Lung elastance. There was no significant difference in lung elastance between the two. D. Inspiratory capacity. There was no significant difference in the lung inspiratory capacity. Data are presented as mean ± standard deviation; N = 2 for S/S and 3 for S/ECM.

5.3.2 Cytology

Cytological differences were measured in the BALF of the S/S and S/ECM groups following lung mechanic measurements. Amongst the percentages of lymphocytes, monocytes, and neutrophils, no statistically significant differences were observed between the S/S and S/ECM groups (Table 1).

Table 1. BALF cellularity. Data presented as the percentage of counted cells. There is no significant difference in the BALF cellularity between the S/S and S/ECM groups. Data are presented as mean ± standard deviation; N = 2 for S/S and 2 for S/ECM.

	S/S	**S/ECM**
Lymphocytes (%)	1.79 ± 0.19	2.83 ± 1.18
Monocytes (%)	97.05 ± 1.45	96.50 ± 1.65
Neutrophils (%)	0.17 ± 0.23	0.33 ± 0.00

5.3.3 Histology

Histology of the S/S and S/ECM lung sections were similar regarding thin alveolar septa and minimal presence of inflammatory cells in the alveolar septa and alveoli (Figure 10).

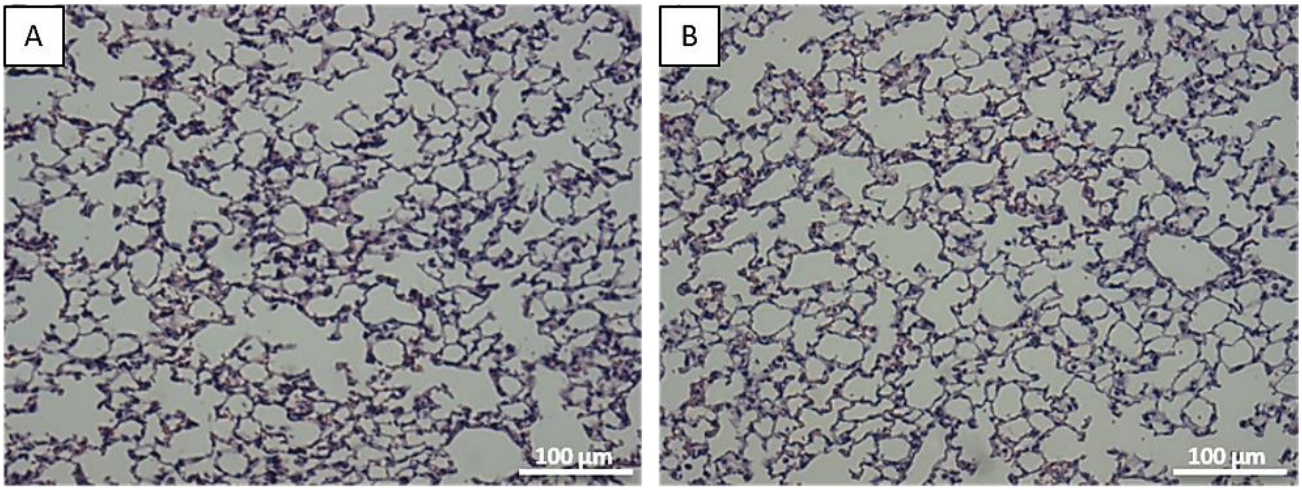

Figure 10. Histological H&E images of A. S/S and B. S/ECM lung sections, respectively. Scale bar is 100 µm.

5.4 Discussion

The results from the *in vivo* study have proven that the ECM nanoparticles do not induce an inflammatory response or unnecessary harm to the lungs when aerosolized IT. There was no statistically significant difference in the lung mechanics or neutrophil cell count between the S/S and S/ECM group. However, it is important to note that this study was preliminary and the n-values of each experiment were low. The n-values of the lung mechanics for S/S was 2 and for S/ECM was 3. The n-values of the BALF cellularity for S/S and S/ECM was 2. Furthermore, the

histological lung sections of both groups showed thin alveolar septa and minimal inflammatory cells in the alveoli.

Lung mechanics indicate the functionality of the lung. In this study, resistance, compliance, elastance, and inspiratory capacity were quantified. Resistance is an indicator for the level of constriction in the lungs; the ease at which air moves through the lungs. Compliance describes the ease at which the lungs expand. Elastance is the opposite of compliance and measures lung stiffness; or resistance to stretch. Inspiratory capacity or total lung capacity is a measure of the amount of air that can be inhaled at the end of expiration.[48, 49] Since the lung mechanics of the S/ECM group were not statistically significant and comparable to the control group, this indicates that the lungs of the S/ECM functioned similarly to normal lungs and that the ECM did not disrupt normal lung function. This is the first known study on lung mechanics using inhaled, decellularized, ECM nanoparticle treatments; however, these lung mechanic results were comparable to C57BL/6 mice that acted as control groups in ventilator induced lung injury models.

A previous study investigating simvastatin as an injurious mechanical ventilation protection for mice showed control group lung resistance, compliance, and elastance data.[50] The lung resistance and elastance of our mice showed slightly lower results compared to this study, which could be due to the IT treatment injections that were used in our study compared to the IP treatment injections of Manitsopoulos et. al. The IT injections of saline could cause insignificant inflammation that could skew the lung mechanic results. The lung compliance, however, was almost identical to the zero timepoint in Manisopoulos et. al..[50] The lung inspiratory capacity of our study is also comparable to a previous study that used a Tpl2 inhibitor as a possible way to

protect against mechanical ventilation-induced lung injury.[51] Similar to the lung resistance and elastance previously discussed, the inspiratory capacity results of our study were slightly lower compared to Kaniaris et. al. This could also possibly be due to the use of IP treatment injections compared to our IT treatment injections, which may cause insignificant lung inflammation.[51]

The recruitment of lymphocytes and neutrophils to the site of injury is part of the normal wound healing process.[47] In ARDS, mentioned in chapter 2, epithelial and endothelial lung injury occurs as a consequence of neutrophil influx.[52] The experimental data from this study revealed that there was no significant difference in the cell counts, as expected based on the lung mechanics. The neutrophil and lymphocyte counts were low in both the control and S/ECM group, indicating no inflammatory response or lung injury caused by the nanoparticles.

The lack of inflammatory cells was also evident in the control and S/ECM histological lung sections and septal thickening, another sign of injury, was not apparent in the S/ECM lung sections, as to be expected. [52] A previous study explored the therapeutic potential of inhaled ECM given intratracheally in an acute lung injury rat model.[35] The hyperoxic rats treated with inhaled ECM showed significantly reduced alveolar septal thickening, tissue edema and cell/fluid exudation, which was evident in their histological lung sections.[35] Although, the study did not have a similar S/ECM group, the inhaled ECM did not cause any harm, which is similar to the results from our study.

Based on the results of this study, aerosolized ECM nanoparticles are not harmful to the lungs *in vivo*.

CHAPTER 6

CONCLUSION & FURTHER DIRECTIONS

We have shown that our ECM nanoparticles do not cause any unwanted harm *in vivo.* The ECM contains tissue-specific components that promote tissue repair and, more specifically, promote epithelial wound repair.[35] ECM may be a potential therapeutic for ARDS because of the ECM's ability to promote tissue repair, which is an advantage to repairing the barrier loss caused by ARDS. However, further studies are needed to show the ECM nanoparticles' therapeutic potential *in vivo*.

Currently, studies are being conducted to determine the distribution of the nanoparticle solution within murine lungs by fluorescently labeling the nanoparticles with Texas Red™ 1,2-Dihexadecanoyl-sn-Glycero-3-Phosphoethanolamine, Triethylammonium Salt (Figure 11).

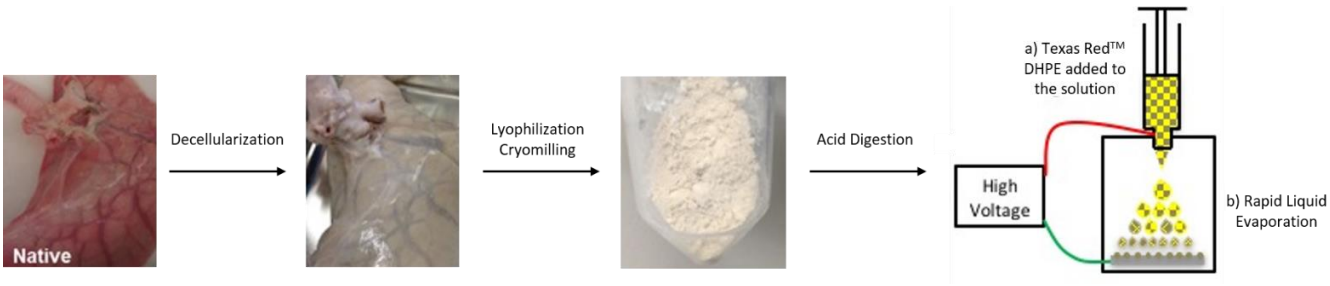

Figure 11. Overview of the process to produce fluorescently labelled ECM nanoparticles.

Further studies are also being done to fully establish an ARDS *in vivo* model to test the effectiveness of the ECM nanoparticles on lung injury. Several studies have been done to establish the timepoints and dosing concentrations for the future ARDS model; however, we are still working on the best ARDS model for this potential treatment.

The *in vivo* study, described in chapter 7, was designed to be used in association with the injurious model using lipopolysaccharide (LPS), which is the reason for the hour timepoint prior to the nanoparticle treatment, but the model has changed drastically since those initial studies.

Establishing the model began by IP injecting 10 mg/kg of LPS into C57BL/6 mice an hour prior to the ECM nanoparticle treatment, at the same 0.125 mg/mL concentration and collecting lung mechanics and BALF at 6, 12, and 24 hours.[53-57] However, we concluded that the IP injections of LPS did not cause enough significant lung injury to lead to an effective ARDS model. It was also concluded that the 12-hour timepoint was the most effective due to the low mice survival rate at the 24-hour timepoint.

Due to the ineffectiveness of the IP injections, we instead used an IT injection at a 2 mg/kg LPS concentration an hour prior to treatment and collected lung mechanics and BALF at 12 hours.[58, 59] We concluded that the IT injections at a 2 mg/kg LPS concentration was effective, but the use of the microsprayer for both IT injections was causing additional, unwanted inflammation in the lungs (Figure 12). Future studies will involve determining if aspirating will be a more effective aerosolization technique that will not cause unwanted inflammation in the lungs.

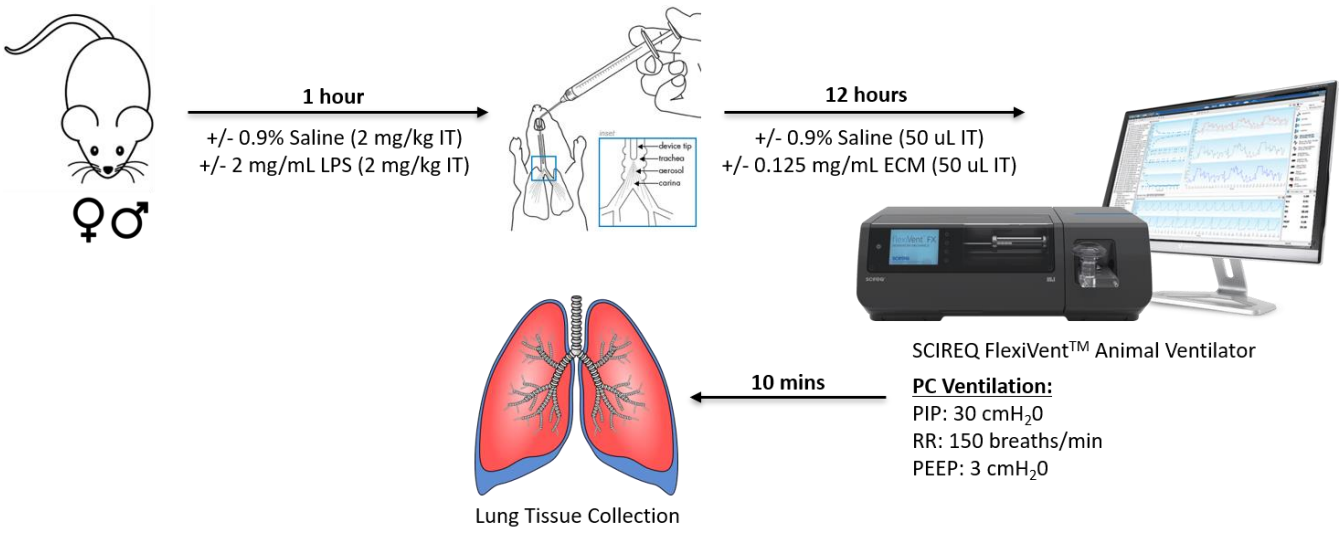

Figure 12. Overview of the injurious model *in vivo* studies testing the effects of the ECM nanoparticle solution at 0.125 mg/mL.

This investigation, nonetheless, demonstrates the potential for the ECM nanoparticles to be used as a therapeutic to treat ARDS, but a large amount of work still needs to be done to fully establish a working ARDS *in vivo* model.

REFERENCES

[1] Costanzo, L. S. (2017) “Physiology: Sixth Edition”. *Elsevier*, pp. 189–191. isbn: 9780323478816.

[2] Patwa, A., & Shah, A. (2015) Anatomy and physiology of respiratory system relevant to anaesthesia. *Indian Journal of Anaesthesia*, 59: 533–541. https://doi.org/10.4103/0019-5049.165849

[3] McNulty, W., & Usmani, O. S. (2014) Techniques of assessing small airways dysfunction. *European Clinical Respiratory Journal*, 1, 10.3402/ecrj.v1.25898. https://doi.org/10.3402/ecrj.v1.25898

[4] Knudsen, L., & Ochs, M. (2018) The micromechanics of lung alveoli: structure and function of surfactant and tissue components. *Histochemistry and Cell Biology*, 150: 661-676. https://doi.org/10.1007/s00418-018-1747-9

[5] OpenStax College (2013) Illustration from Anatomy & Physiology. *Anatomy & Physiology*. http://cnx.org/content/col11496/1.6/

[6] Berthiaume, Y., Voisin, G., & Dagenais, A. (2006) The alveolar type I cells: the new knight of the alveolus? *The Journal of Physiology*, 572 (Pt 3): 609–610. https://doi.org/10.1113/jphysiol.2006.109579

[7] Ward, H. E., & Nicholas, T. E. (1984) Alveolar type I and type II cells. *Aust N Z J Med*, 14: 731-734.

[8] Wang, Y., Tang, Z., Huang, H., Li, J., Wang, Z., Yu, Y., Zhang, C., Li, J., Dai, H., Wang, F., Cai, T., & Tang, N. (2018) Pulmonary alveolar type I cell population consists of two distinct subtypes

that differ in cell fate. *Proceedings of the National Academy of Sciences*, 115 (10): 2407. https://doi.org/10.1073/pnas.1719474115

[9] Bernhard, W. (2016) Lung surfactant: Function and composition in the context of development and respiratory physiology. *Annals of Anatomy – Anatomischer Anazeiger*, 208: 146-150. https://doi.org/10.1016/j.aanat.2016.08.003

[10] White, E. (2014) Lung extracellular matrix and fibroblast function. *Annals of the American Thoracic Society*, 12. https://doi.org/10.1513/AnnalsATS.201406-240MG

[11] Annoni, R., Lancas, T., Tanigawa, R., Matsushita, M., Fernezlian, S., Bruno, A., Silva, L., Roughley, P., Battaglia, S., Dolhnikoff, M., Hiemstra, P., Sterk, P., Rabe, K., & Mauad, T. (2012). Extracellular matrix composition in COPD. *European Respiratory Journal,* 40: 1362-1373. DOI: 10.1183/09031936.00192611

[12] Burgstaller, G., Oehrle, B., Gerckens, M., White, E., Schiller, H., & Eickelberg, O. (2017) The instructive extracellular matrix of the lung: basic composition and alterations in chronic lung disease. *European Respiratory Journal*, 50: 1601805. DOI: 10.1183/13993003.01805-2016

[13] Raghu, G., Striker, L., Hudson, L., & Striker, G. (1983) Extracellular matrix in normal and fibrotic human lungs. *American Review of Respiratory Disease,* 131 (2).

[14] Frantz, C., Stewart, K. M., & Weaver, V. M. (2010) The extracellular matrix at a glance. *Journal of Cell Science*, 123: 4195-4200. doi: 10.1242/jcs.023820

[15] Phua, J., Badia, J. R., Adhikari, N. K. J., Friedrich, J. O., Fowler, R. A., Singh, J. M., Scales, D. C., Stather, D. R., Li, A., Jones, A., Gattas, D. J., Hallett, D., Tomlinson, G., Stewart, T. E., & Ferguson, N. D. (2009) Has mortality from acute respiratory distress syndrome decreased over

time? A systemic review. *American Journal of Respiratory and Critical Care Medicine*, 179: 220-227. https://doi.org/10.1164/rccm.200805-722OC

[16] Matthay, M. A., & Zemans, R. L. (2011) The acute respiratory distress syndrome: pathogenesis and treatment. *Annual Review of Pathology*, 6: 147–163. https://doi.org/10.1146/annurev-pathol-011110-130158

[17] Udobi, K. F., Childs, E., & Touijer, K. (2003) Acute respiratory distress syndrome. *Am Fam Physician*, 67(2): 315-322.

[18] Sharp, C., Millar, A. B., & Medford, A. R. L. (2015) Advances in understanding of the pathogenesis of acute respiratory distress syndrome. *Respiration*, 89: 420-434. https://doi.org/10.1159/000381102

[19] Huang, X., Xiu, H., Zhang, S., & Zhang, G. (2018) The role of macrophages in the pathogenesis of ALI/ARDS. *Mediators of Inflammation*, 2018, 1264913. https://doi.org/10.1155/2018/1264913

[20] Saqib, U., Sarkar, S., Suk, K., Mohammad, O., Baig, M. S., & Savai, R. (2018) Phytochemicals as modulators of M1-M2 macrophages in inflammation. *Oncotarget*, 9 (25): 17937–17950. https://doi.org/10.18632/oncotarget.24788

[21] Ley, K. (2017) M1 means kill; M2 means heal. *The Journal of Immunology*, 199 (7): 2191-2193. https://doi.org/10.4049/jimmunol.1701135

[22] Borregaard, N. (2010) Neutrophils, from marrow to microbes. *Immunity*, 33: 657-670. https://doi.org/10.1016/j.immuni.2010.11.011

[23] Timlin, M., Toomey, D., Condron, C., Power, C., Street, J., Murray, P., & Bouchier-Hayes, D. (2005) Fracture hematoma is a potent proinflammatory mediator of neutrophil function. *The Journal of Trauma and Acute Care* Surgery, 58: 1223-1229.

[24] Morales, M.M., Pires-Neto, R.C., Inforsato, N., Lancas, T., Silva, L., Saldiva, P., Carvalho, C., Amato, M., & Dolhnikoff, M. (2011) Small airway remodeling in acute respiratory distress syndrome: a study in autopsy lung tissue. *Critical Care,* 15: R4. https://doi.org/10.1186/cc9401

[25] Brower, R. G., Ware, L. B., Bethiaume, Y., & Matthay, M. A. (2001) Treatment of ARDS. *CHEST*, 120: 1347-1367.

[26] Diamond, M., Peniston Feliciano, H. L., Sanghavi, D., & Mahapatra, S. (2020) Acute respiratory distress syndrome (ARDS). *StatPearls.* https://www.ncbi.nlm.nih.gov/books/NBK436002/

[27] Pouliot, R., Mikhaiel, N., Wong, B., & Heise, R. (2015). Extracellular matrix hydrogels from decellularized lung tissue. http://abstracts.biomaterials.org/data/papers/2015/abstracts/721.pdf

[28] Pouliot, R., Link, P., Mikhaiel, N., Schneck, M., Valentine, M., Gninzeko, F., Herbert, J., Sakagami, M., & Heise, R. (2016) Development and characterization of a naturally derived lung extracellular matrix hydrogel. *Journal of Biomedical Materials Research*, 104 (8): 1922-1935. https://doi.org/10.1002/jbm.a.35726

[29] Li, F., Li, W., Johnson, S. A., Ingram, D. A., Yoder, M. C., & Badylak, S. F. (2004) Low-molecular-weight peptides derived from extracellular matrix as chemoattractants for primary endothelial cells. *Endothelium: Journal of Endothelial Cell Research*, 11: 199-206. https://doi.org/10.1080/10623320490512390

[30] Zantop, T., Gilbert, T. W., Yoder, M. C., & Badylak, S. F. (2006) Extracellular matrix scaffolds are repopulated by bone marrow-derived cells in a mouse model of achilles tendon reconstruction. *Journal of Orthopaedic Research*, 24: 1299-1309. https://doi.org/10.1002/jor.20071

[31] Reing, J. E., Zhang, L., Myers-Irvin, J., Cordero, K. E., Freytes, D. O., Heber-Katz, E., Bedelbaeva, K., McIntosh, D., Dewilde, A., Braunhut, S. J., & Badylak, S. F. (2009) Degradation product of extracellular matrix affect cell migration and proliferation. *Tissue Engineering Part A,* 15: 605-614. http://doi.org/10.1089/ten.tea.2007.0425

[32] Sarikaya, A., Record, R., Wu, C., Tullius, B., Badylak, S., & Ladisch, M. (2002) Antimicrobial activity associated with extracellular matrices.*Tissue Engineering Part A*, 8: 63-71. http://doi.org/10.1089/107632702753503063

[33] Link, P. A., Ritchie, A. M., Cotman, G. M., Valentine, M. S., Dereski, B. S., Heise, R. L. (2018) Electrosprayed extracellular matrix nanoparticles induce a pro-regenerative cell response. *Journal of Tissue Engineering and Regenerative Medicine*, 12: 2331-2336. https://doi.org/10.1002/term.2768

[34] Manni, M. L., Czajka, C. A., Oury, T. D., & Gilbert, T. W. (2011) Extracellular matrix powder protects against bleomycin-induced pulmonary fibrosis. *Tissue Engineering Part A*, 17: 2795-2804. https://doi.org/10.1089/ten.tea.2011.0023

[35] Wu, J., Ravikumar, P., Nguyen, K. T., Hsia, C. C. W., & Hong, Y. (2017) Lung protection by inhalation of exogenous solubilized extracellular matrix. *PLoS ONE,* 12: e0171165. https://doi.org/10.1371/journal.pone.0171165

[36] Labiris, N. R. & Dolovich, M. B. (2003) Pulmonary drug delivery. Part II: The role of inhalant delivery devices and drug formulations in therapeutic effectiveness of aerosolized medications. *British Journal of Clinical Pharmacology*, 56: 600-612. https://doi.org/10.1046/j.1365-2125.2003.01893.x

[37] Anderson, P. J. (2001) Delivery options and devices for aerosolized therapeutics. *CHEST*, 120: 89S-93S. https://doi.org/10.1378/chest.120.3_suppl.89S

[38] Mitchell, J.P., Nagel, M.W., Wiersema, K.J., & Doyle, C. C. (2003) Aerodynamic particle size analysis of aerosols from pressurized metered-dose inhalers: Comparison of andersen 8-stage cascade impactor, next generation pharmaceutical impactor, and model 3321 aerodynamic particle sizer aerosol spectrometer. *AAPS PharmSciTech*, 4: 425-433. https://doi.org/10.1208/pt040454

[39] Peng, T., Lin, S., Niu, B., Wang, X., Huang, Y., Zhang, X., Li, G., Pan, X., & Wu, C. (2016) Influence of physical properties of carrier on the performance of dry powder inhalers. *Acta pharmaceutica Sinica. B*, 6: 308-318. https://doi.org/10.1016/j.apsb.2016.03.011

[40] Heyder, J., Gebhart, J., Rudolf, G., Schiller, C. F., & Stahlhofen, W. (1986) Deposition of particles in the human respiratory tract in the size range 0.005–15 µm. *Journal of Aerosol Science*, 17: 811-825. https://doi.org/10.1016/0021-8502(86)90035-2

[41] Asgharian, B., Kelly, J. T., & Tewksbury, E. W. (2003) Respiratory deposition and inhalability of monodisperse aerosols in Long-Evans rats. *Toxicological Sciences*, 71: 104-111. https://doi.org/10.1093/toxsci/71.1.104

[42] Byron, P.R. (1986) Prediction of drug residence times in regions of the human respiratory tract following aerosol inhalation. *Journal of Pharmaceutical Sciences*, 75: 433-438. https://doi.org/10.1002/jps.2600750502

[43] Young, B. M., Shankar, K., Tho, C. K., Pellegrino, A. R., & Heise, R. L. (2019) Laminin-driven Epac/Rap1 regulation of epithelial barriers on decellularized matrix. *Acta Biomaterialia*, 200: 223-234. https://doi.org/10.1016/j.actbio.2019.10.009

[44] Molina, R. M., Konduru, N. V., Hirano, H., Donaghey, T. C., Adamo, B., Laurenzi, B., Pyrgiotakis, G., & Brain, J. D. (2016) Pulmonary distribution of nanoceria: comparison of intratracheal, microspray instillation and dry powder insufflation. *Inhalation toxicology*, 28: 550-560. https://doi.org/10.1080/08958378.2016.1226449

[45] Bivas-Benita, M., Zwier, R., Junginger, H. E., & Borchard, G. (2005) Non-invasive pulmonary aerosol delivery in mice by the endotracheal route. *European Journal of Pharmaceutics and Biopharmaceutics*, 61: 214-218. https://doi.org/10.1016/j.ejpb.2005.04.009

[46] https://www.manualsdir.com/manuals/340966/penn-century-ia-1b-r-for-rat-ia-1b-gp-for-guinea-pig-ia-1b-c-for-custom-lengths.html?page=3

[47] Herbert, J. A., Valentine, M. S., Saravanan, N., Schneck, M. B., Pidaparti, R., Fowler, A. A., 3rd, Reynolds, A. M., & Heise, R. L. (2016) Conservative fluid management prevents age-associated ventilator induced mortality. *Experimental gerontology*, 81: 101-109. https://doi.org/10.1016/j.exger.2016.05.005

[48] Desai, J. P. & Moustarah, F. (2019) Pulmonary compliance. *StatsPearls*. https://www.ncbi.nlm.nih.gov/books/NBK538324/#_NBK538324_pubdet_

[49] Bates, J. H. T. & Irvin, C. G. (2003) Measuring lung function in mice: the phenotyping uncertainty principle. *Journal of Applied Physiology*, 94: 1297-1306. https://doi.org/10.1152/japplphysiol.00706.2002

[50] Manitsopoulos, N., Orfanos, S.E., Kotanidou, A., Nikitopoulou, I., Siempos, I., Magkou, C., Dimopoulou, I., Zakynthinos, S., Armaganidis, A., & Maniatis, N. (2015) Inhibition of HMGCoA reductase by simvastatin protects mice from injurious mechanical ventilation. *Respiratory Research,* 16: 24. https://doi.org/10.1186/s12931-015-0173-y

[51] Kaniaris, E., Vaporidi, K., Vergadi, E., Theodorakis, E., Kondili, E., Lagoudaki, E., Tsatsanis, C., & Georgopoulos, D. (2014) Genetic and pharmacologic inhibition of Tpl2 kinase is protective in a mouse model of ventilator-induced lung injury. *Intensive Care Medicine Experimental*, 2: 15. https://doi.org/10.1186/2197-425X-2-15

[52] Costa, N., Junior, G. R., Alemany, A., Belotti, L., Zati, D. H., Cavalcante, M. F., Veras, M. M., Ribeiro, S., Kallas, E. G., Saldiva, P., Dolhnikoff, M., & Silva, L. (2017) Early and late pulmonary effects of nebulized LPS in mice: An acute lung injury model. *PloS One*, 12: e0185474. https://doi.org/10.1371/journal.pone.0185474

[53] Fu, J., Zang, Y., Zhou, Y., Chen, C., Shao, S., Hu, M., Shi, G, Wu, L., Zhang, D., & Zhang, T. (2020) A novel triptolide derivative ZT01 exerts anti-inflammatory effects by targeting TAK1 to prevent macrophage polarization into pro-inflammatory phenotype. *Biomedicine & Pharmacotherapy*, 126: 110084. https://doi.org/10.1016/j.biopha.2020.110084

[54] Lew, W. Y., Bayna, E., Molle, E. D., Dalton, N. D., Lai, N. C., Bhargava, V., Mendiola, V., Clopton, P., & Tang, T. (2013) Recurrent exposure to subclinical lipopolysaccharide increases

mortality and induces cardiac fibrosis in mice. PloS one, 8: e61057. https://doi.org/10.1371/journal.pone.0061057

[55] Fairchild, K. D., Saucerman, J. J., Raynor, L. L., Sivak, J. A., Xiao, Y., Lake, D. E., & Moorman, J. R. (2009). Endotoxin depresses heart rate variability in mice: cytokine and steroid effects. *American Journal of Physiology: Regulatory, Integrative and Comparative Physiology*, 297: R1019-R1027. https://doi.org/10.1152/ajpregu.00132.2009

[56] Schock, B. C., Vliet, A., Corbacho, A. M., Leonard, S. W., Finkelstein, E., Valacchi, G., Obermueller-Jevic, U., Cross, C. E., & Traber, M. G. (2004) Enhanced inflammatory responses in α-tocopherol transfer protein null mice. *Archives of Biochemistry and Biophysics*, 423: 162-169. https://doi.org/10.1016/j.abb.2003.12.009

[57] Kawasaki, M., Kuwano, K., Hagimoto, N., Matsuba, T., Kunitake, R., Tanaka, T., Maeyama, T., & Hara, N. (2000) Protection from Lethal Apoptosis in Lipopolysaccharide-Induced Acute Lung Injury in Mice by a Caspase Inhibitor. *The American Journal of Pathology*, 157: 597-603. https://doi.org/10.1016/S0002-9440(10)64570-1

[58] Yue, X., & Guidry, J. J. (2019) Differential Protein Expression Profiles of Bronchoalveolar Lavage Fluid Following Lipopolysaccharide-Induced Direct and Indirect Lung Injury in Mice. *International journal of molecular sciences*, 20: 3401. https://doi.org/10.3390/ijms20143401

[59] D'Alessio F.R. (2018) Mouse Models of Acute Lung Injury and ARDS. *Lung Innate Immunity and Inflammation,* 1809. https://doi.org/10.1007/978-1-4939-8570-8_22

VITA

Brittaney Elizabeth Ritchie was born on September 15, 1994 in Fort Campbell, Kentucky and is an American citizen. She graduated from Freedom High School, South Riding, Virginia in 2012. She received her Bachelor of Science in Biology from Randolph-Macon College, Ashland, Virginia in 2016, where she started her research career studying the olfactory bulb of mice in 2013. She went on to Johns Hopkins to study treatments for pediatric central nervous system tuberculosis for an additional two years prior to entering Virginia Commonwealth University to pursue a Master's Degree.